Unclassified

SECURITY CLASSIFICATION OF THIS PAGE (When Data Entered)

| REPORT DOCUMENTATION PAGE | | READ INSTRUCTIONS BEFORE COMPLETING FORM |
|---|---|---|
| 1. REPORT NUMBER<br>AFGL-TR-83-0097 | 2. GOVT ACCESSION NO.<br>AD A127007 | 3. RECIPIENT'S CATALOG NUMBER |
| 4. TITLE (and Subtitle)<br>EMPIRICAL MODELING OF THE GEOMAGNETIC VARIATION IN THE THERMOSPHERE* | | 5. TYPE OF REPORT & PERIOD COVERED<br>Reprint<br>6. PERFORMING ORG. REPORT NUMBER |
| 7. AUTHOR(s)<br>JACK W. SLOWEY | | 8. CONTRACT OR GRANT NUMBER(s)<br>F19628-81-K-0033 |
| 9. PERFORMING ORGANIZATION NAME AND ADDRESS<br>SMITHSONIAN ASTROPHYSICAL OBSERVATORY<br>60 GARDEN STREET<br>CAMBRIDGE, MA 02138 | | 10. PROGRAM ELEMENT, PROJECT, TASK AREA & WORK UNIT NUMBERS<br>PE 62101F, T669008<br>W.U. 669007AJ |
| 11. CONTROLLING OFFICE NAME AND ADDRESS<br>AIR FORCE GEOPHYSICS LABORATORY<br>HANSCOM AFB, MA 01731<br>MONITOR: DOROTHY F. GILLETTE/LKB/3037 | | 12. REPORT DATE<br>May, 1982<br>13. NUMBER OF PAGES<br>11 |
| 14. MONITORING AGENCY NAME & ADDRESS (if different from Controlling Office) | | 15. SECURITY CLASS. (of this report)<br>Unclassified<br>15a. DECLASSIFICATION/DOWNGRADING SCHEDULE |

16. DISTRIBUTION STATEMENT (of this Report)

Approved for public release; distribution unlimited.

17. DISTRIBUTION STATEMENT (of the abstract entered in Block 20, if different from Report)

18. SUPPLEMENTARY NOTES

*Reprint from "Proceedings of a Workshop on Satellite Drag", Space Environment Services Center, Space Environment Laboratory, Boulder, CO, May, 1982

19. KEY WORDS (Continue on reverse side if necessary and identify by block number)

Empirical model
Geomagnetic variation
Thermosphere
Exosphere



20. ABSTRACT (Continue on reverse side if necessary and identify by block number)

See attached Abstract

DD FORM 1473, 1 JAN 73 EDITION OF 1 NOV 65 IS OBSOLETE

Unclassified

SECURITY CLASSIFICATION OF THIS PAGE (When Data Entered)

83 04 19 039

**Abstract.** This paper briefly summarizes the development of empirical models of the geomagnetic variation in the thermosphere and exosphere. The earliest models were based exclusively on the results of satellite drag analysis. Although they present a much simplified picture of what is an extremely complex phenomenon, these models are still valid in many applications and remain in wide use. They do, however, leave much to be desired with respect to short-term accuracy and are quite inadequate in many cases in the way in which they depict local conditions. More recent observational data, particularly those from satellite-borne gas analyzers, have resulted in a considerable improvement in empirical models of the geomagnetic variation. One such model and its limitations are described in some detail. Some of the problems relating to the development of improved models in the future are also examined.

# II.2 EMPIRICAL MODELING OF THE GEOMAGNETIC VARIATION IN THE THERMOSPHERE

Jack W. Slowey

Center for Astrophysics
Harvard College Observatory
and
Smithsonian Astrophysical Observatory

Cambridge, Massachusetts 02138

Abstract. This paper briefly summarizes the development of empirical models of the geomagnetic variation in the thermosphere and exosphere. The earliest models were based exclusively on the results of satellite drag analysis. Although they present a much simplified picture of what is an extremely complex phenomenon, these models are still valid in many applications and remain in wide use. They do, however, leave much to be desired with respect to short-term accuracy and are quite inadequate in many cases in the way in which they depict local conditions. More recent observational data, particularly those from satellite-borne gas analyzers, have resulted in a considerable improvement in empirical models of the geomagnetic variation. One such model and its limitations are described in some detail. Some of the problems relating to the development of improved models in the future are also examined.

## 1. MODELS BASED ON DRAG ANALYSIS

Heating of the neutral atmosphere in association with magnetic storms was suggested by many early studies of ionospheric disturbance and the aurorae. There was, however, no direct evidence of such heating until Jacchia (1959, 1961) detected a correlation between magnetic storms and short-lived increases in the atmospheric drag on artificial satellites. Following this discovery, the results of drag analysis were used extensively to study the variation of the atmosphere with geomagnetic activity and were, for a long time, the only significant source of information on the subject. These studies led to the development of simple empirical models of the geomagnetic variation (Jacchia and Slowey, 1964a, 1964b; Jacchia et al., 1967; Roemer, 1971) which, by inclusion in one or another of the early comprehensive models of the heterosphere (thermosphere and exosphere), are still widely used, particularly in relation to problems of satellite orbital analysis and ephemeris prediction. This phase in the development of models of the geomagnetic variation is summarized in reviews by Jacchia (1972) and Roemer (1972) published with the 1972 COSPAR reference atmosphere (CIRA 1972).

The models derived from satellite drag usually consisted of an equation relating an increase in the exospheric temperature of the atmosphere to the planetary geomagnetic index $a_p$ or to its quasi-logarithmic equivalent $K_p$. The corresponding density at any height was then to be obtained by entering the augmented exospheric temperature in a static diffusion model of the atmosphere. The implicit assumption was that the shape of the temperature profiles during geomagnetic disturbances was unchanged with respect to the static models. Actually, of course, one would expect the profiles to be considerably distorted in the vicinity of the lower thermospheric heat sources that drive the geomagnetic variation. Still, the models represented the observed density variations at heights above 200 km rather well. Below 200 km, however, it was necessary to introduce an added relative increase directly in the density in order to compensate for the limited sensitivity of the static models at lower heights to variations in the exospheric temperature input (Jacchia, 1972).

The orbital-drag method does not provide high resolution, either spatially or temporally, and this was a considerable disadvantage in the case of the geomagnetic variation. Time resolution as short as 0.1 day has been achieved in drag work (Jacchia and Slowey, 1963) but a resolution of 0.20 - 0.25 day during large magnetic storms is more typical of the data from orbit analysis. During quieter periods, even the smallest variations with geomagnetic activity can be detected (Jacchia and Slowey, 1964b) but the resolution of these is poorer still. And, since the drag effect cannot be resolved within a single orbital period, the derived density necessarily represents an average over a fairly long arc of the orbit on either side of perigee. Thus, the data from orbital-drag analysis could only give a smoothed picture of a phenomenon that turned out to be quite complex in form. This complexity became obvious with the first high-resolution measurements of densities and composition with satellite-borne accelerometers (DeVries, 1972) and gas analyzers (i.e., neutral mass spectrometers) (Taeusch et al., 1971).

Although most of the models based on orbital drag assumed the geomagnetic variation to be uniform over the globe, several important details of the variation did emerge from drag analysis, albeit in rudimentary form. Jacchia and Slowey (1964a) and Jacchia et al. (1967) reported that, on occasion, the geomagnetic variation was substantially enhanced in the auroral zones. Roemer (1971) did, in fact, modify the model of Jacchia et al. (1967) to include a latitude dependence. Roemer (1971) was also able to detect a sinusoidal dependence of the geomagnetic variation on local time, with a maximum in the relative temperature increase at 3 am larger by a factor of 1.30 with respect to a 3 pm minimum. Jacchia and Slowey (1964a) also found an increase in the time lag between a geomagnetic disturbance and its atmospheric counterpart in going from high to low latitudes. This and the observed enhancement in high latitudes were evidence of the transport of energy from high to low latitudes during magnetic storms, a fact later corroborated by observations of winds (Smith, 1968; Hays and Roble, 1976) and gravity waves (Newton et al., 1969; Champion et al., 1970) in the thermosphere.

## 2. RECENT MODELS

Data from satellite-borne gas analyzers revolutionized the study of the upper atmosphere and, in particular, the geomagnetic variation. Data from accelerometers have also been important because of their greatly improved resolution as opposed to orbital-drag analysis. The gas-analyzer results, however, provide information on composition in addition to improved resolution. Changes in the neutral composition associated with geomagnetic disturbance turn out to be extremely important in understanding the physical processes involved in the geomagnetic variation.

Spherical harmonic models, patterned after the original OGO 6 model of Hedin et al. (1974), have been fitted to the data from a number of the gas-analyzer experiments. Some of these include (geographic) latitude dependent terms for the geomagnetic variation (usually as a function of the daily $A_p$ index) while some, such as the ESRO 4 model of von Zahn et al. (1977), are specifically fitted only to data corresponding to geomagnetically quiet conditions. The most prominent of the spherical harmonic models is the MSIS model of Hedin et al. (1977a, 1977b) that was fitted to gas-analyzer data from five different satellite experiments as well as neutral temperatures inferred from incoherent scatter measurements made at a number of ground stations. This model was extended by Hedin et al. (1979) to include longitude/UT variations. We cannot discuss these models in detail here but, instead, refer the reader to recent reviews such as that by Prölss (1980). We shall, however, describe in some detail the model of the geomagnetic variation that was derived from ESRO 4 gas-analyzer data by Jacchia et al. (1976, 1977) and incorporated in Jacchia's most recent comprehensive model of the heterosphere (Jacchia, 1977).

The model of Jacchia et al. represents the geomagnetic variation as a function of the geomagnetic latitude, averaged over local time and other conditions, and the $K_p$ index. Density and composition changes under geomagnetically disturbed conditions are reproduced by an increase in exospheric temperature and a proportional increase in the height of the homopause. The later is a convenient device to account for an effect that seems more likely to be due to wind-induced vertical diffusion. Superimposed on these two effects is an 'equatorial wave' in which the number densities of all constituents increase *in the same proportion* and that propagates into low latitudes. The change in the logarithm of the number density of the species i, $\Delta_G \log n_i$, is thus assumed to be given by the sum of three separate components,

$$\Delta_G \log n_i = \Delta_T \log n_i + \Delta_H \log n_i + \Delta_e \log n_i \qquad (1)$$

where $\Delta_T \log n_i$ is the thermal component, $\Delta_H \log n_i$ is the component due to the change in the height of the homopause and $\Delta_e \log n_i$ is the component due to the equatorial wave.

The thermal component of the variation $\Delta_T \log n_i$ is evaluated from an exospheric temperature increase $\Delta_G T_\infty$ given by .

$$\Delta_G T_\infty = A \sin^4 \phi \qquad (2)$$

where $\phi$ is the geomagnetic (preferably the invariant) latitude and the polar amplitude A is given by

$$A = 57.5° K_p' \; [1 + 0.027 \exp (0.4 \; K_p')] \qquad (3)$$

where $K_p'$ is the $K_p$ index at a time $t - \tau$, and $\tau$ is given by

$$\tau = 0.1 + 0.2 \cos^2 \phi \quad \text{(day)}. \qquad (4)$$

For heights in the lower thermosphere, the temperature profiles of the static models are to be incremented by an amount given by (Jacchia, 1977)

$$\Delta_G T(z) = \Delta_G T_\infty \tanh [c(z-z_0)], \qquad (5)$$

where $c = 0.006$ and $z_0 = 90$ km. The disturbed temperature profiles defined by equation (5) yield species densities that are in good agreement with observations at heights as low as 150 km. Analytical expressions, derived from the results of numerical integration of the disturbed profiles, are available from which $\Delta_T \log n_i$, including the effect of equation (5), can be computed directly.

The component due to the change in the height of the homopause is given by

$$\Delta_H \log n_i = \alpha_i \, \Delta z_H \,, \tag{6}$$

where $\Delta z_H$ (meters) is computed from

$$\Delta z_H = 5.0 \times 10^3 \sinh^{-1}(0.010 \Delta_G T_\infty) \tag{7}$$

and the $\alpha_i$ are:

$$\begin{aligned} \alpha(Ar) &= +3.07 \times 10^{-5} \quad (\text{mks}) \\ \alpha(O_2) &= +1.03 \times 10^{-5} \quad (\text{mks}) \\ \alpha(N_2) &= \phantom{+}0.0 \\ \alpha(O) &= -4.85 \times 10^{-5} \quad (\text{mks}) \\ \alpha(He) &= -6.30 \times 10^{-5} \quad (\text{mks}). \end{aligned} \tag{8}$$

With the exception of the value for O, these values of $\alpha_i$ were determined numerically from the static models. The value for O was determined by observation and is about 20% larger than that computed from the models. This is not surprising since oxygen dissociation is still important at the height of the homopause, so that O is very far from being in diffusion equilibrium.

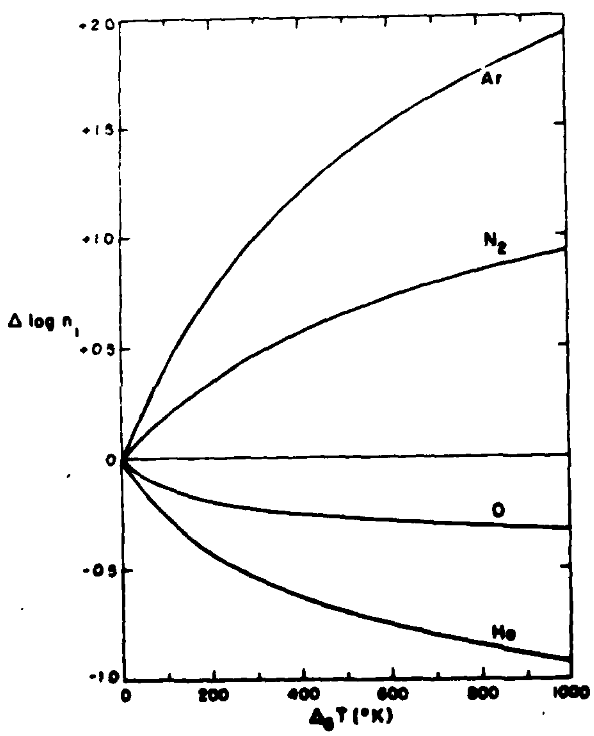


Figure 1. Variation in the densities of Ar, $N_2$, O, and He at 280 km as a function of geomagnetic heating for a 'quiet' exospheric temperature of 900 K.

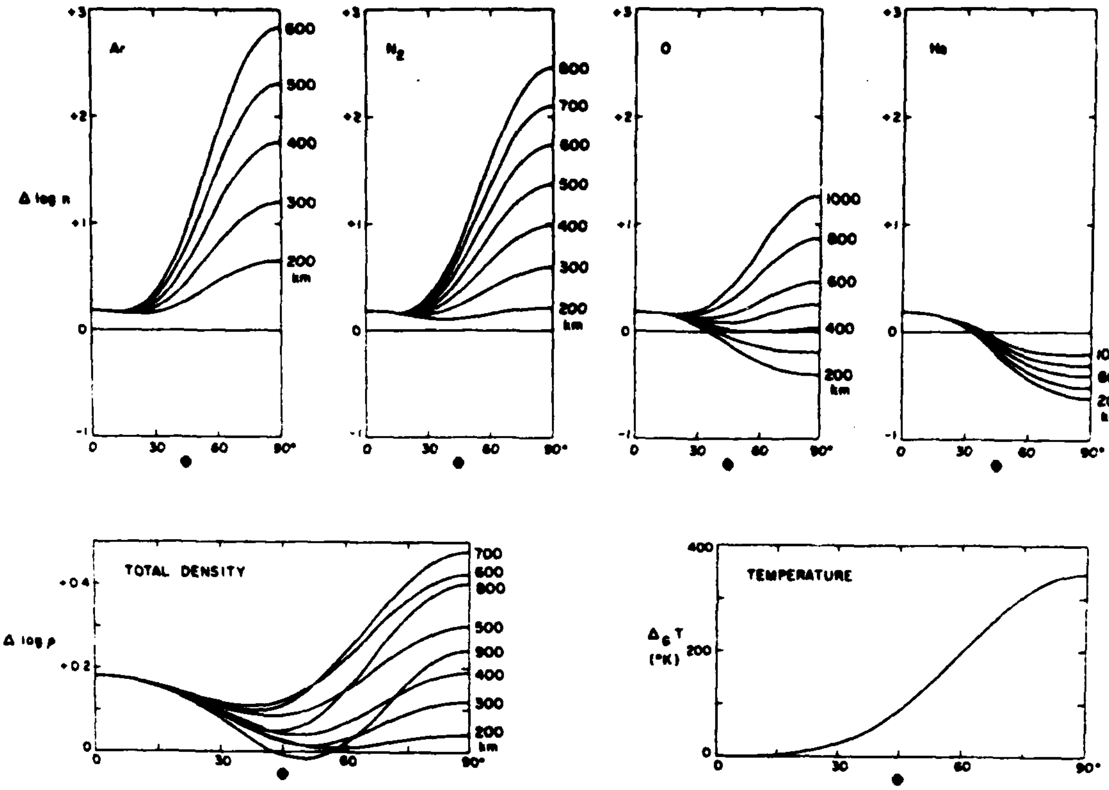


Figure 2. Latitudinal profiles of Ar, $N_2$, O, and He number densities and of total atmospheric density at various heights for $K_p' = 5$ and a 'quiet' exospheric temperature of 900 K. The profile of the exospheric temperature increase is also shown.

The component due to the equatorial wave is assumed to depend on the temperature amplitude of the disturbance given by equation (3) and is represented by

$$\Delta_e \log n_i = \Delta_e \log \rho = 5.2 \times 10^{-4} A \cos^4 \Phi \qquad (9)$$

where $\rho$ is the total density. This component, which is a clear and significant part of the geomagnetic variation, is not, to our knowledge, included in other models.

The nature of the variations predicted by the model are shown in Figures 1-3. In Figure 1, the variations of four atmospheric constituents at a height of 280 km are shown as a function of $\Delta_G T_\infty$. The variations are those at the poles and represent only the effects of the thermal increase and the increase in the height of the homopause. As can be seen, the effect of the thermal increase at this height is insufficient to overcome the effect of the increase in the height of the homopause on the lighter constituents, O and He, and the densities of these constituents decrease rather than increase in response to geomagnetic disturbance. In Figure 2, the variations of the same constituents and the total density are shown for various heights, together with the variation in exospheric temperature, as a function of the geomagnetic latitude for $K_p' = 5$ (A = 345 K). Here, the density variations include the effects of all three components of the model. The variation in total density at different heights does, of course, depend on the composition at that height. At moderate heights, where O is the major atmospheric constituent, the variation in the total density closely follows that of O. At lower heights, the variation in total density is also effected by the variation in $N_2$. This is especially true in high latitudes because of the large increase in exospheric temperature. At greater heights, where He begins to become the major constituent, the variation in total density is increasingly effected by the variation in He. Thus, the relative amplitude of the variation in total density attains a maximum at about 700 km and then begins to decrease. In Figure 3, profiles of the total exospheric temperature around the meridional circle containing $17^h$ and $5^h$ local time are shown for both equinox and solstice conditions. It is clear from the figure that even moderate geomagnetic activity can shift the global maximum in exospheric temperature from its 'quiet' position into much higher latitudes.

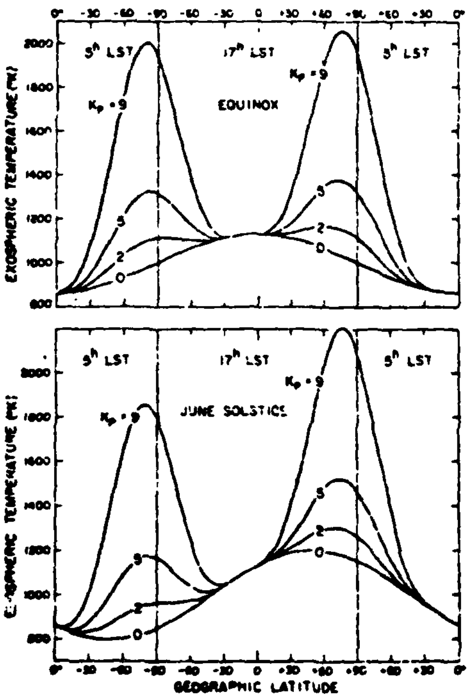


Figure 3. Exospheric temperature profiles along the $17^h$– $5^h$ local time meridian for various levels of geomagnetic activity.

## 3. LIMITATIONS OF THE MODEL

One limitation of the model that has been described here is that it was derived primarily from data at the single height of 280 km. While the model has been shown to work rather well in the lower thermosphere, it has not been tested at greater heights. This is a matter of some concern in view of the large relative amplitudes that the model predicts at greater heights. There is also evidence from comparisons with satellite drag that, even in the vicinity of 280 km, the dip in the latitudinal response of the total density in mid-latitudes is exaggerated in the model. Jacchia and Slowey (1981) have made a preliminary revision to the model based on re-examination of the ESRO 4 data in which both the exospheric temperature increase centered on the poles and the equatorial wave are somewhat broadened. The main effect of this revision is to increase the positive response of atomic oxygen and, hence, that of the total density at lower heights in mid-latitudes.

The model also does not allow for a variation in the shape of the latitudinal response with the intensity of the disturbance. Such changes have been observed in the ESRO 4 data by Prölss and Fricke (1976) and by Slowey (1981) and seem to be related to variations in the positions of the energy sources heating the atmosphere. The latitudinal position of the polar cusp region, for example, varies by 15 degrees or more in response to intensity variation of the ring current as indicated by the Dst index (Meng, 1982).

In addition, the time lag between a geomagnetic disturbance and the associated atmospheric perturbation specified by the model, is, on average, probably too large. Here we were guided more by the results from orbital-drag analysis than the gas-analyzer data. It is increasingly evident that response times are extremely short in high latitudes (Taeusch et al., 1971; Prölss and Fricke, 1976) and may be as little as 3-4 hours in the equatorial region (Slowey, unpublished), at least with respect to the AE geomagnetic index. Much work remains to be done, however, both on the possible variability of the time delay and the applicability of different activity indices to the geomagnetic variation.

A related, though considerably more difficult, question is that of the persistence of the effects of atmospheric perturbation. The heating involved in a geomagnetic disturbance results in a large-scale transport of mass and energy (see, for example, Fuller-Rowell and Rees, 1981) and the winds and waves associated with the disturbance will persist for a considerable period after the heat input ceases. Porter et al. (1981), have recently developed an empirical formulation for the effects of disturbance that incorporates the prior history of the heat input. This has been applied to the analysis of two disturbed periods by Hedin et al. (1981) with good results and seems to be a step in the right direction. A much simpler approach would, however, seem to be required for most practical applications.

## 4. FUTURE DEVELOPMENT

The most formidable problem remaining in the development of empirical models of the geomagnetic variation is that of the realistic representation of local time effects, while at the same time taking into account whatever dependence on longitude and on season as may exist. Some idea of the complexity involved in modeling the local time effects can be seen in Figure 4, which shows relative isotherms of the exospheric temperature increase plotted as a function of geomagnetic latitude and local time in the region poleward of 30 degrees latitude. The exospheric temperatures used to draw the figure were obtained by inversion of the $N_2$ densities measured by ESRO 4 at a height of 280 km under the assumption that $N_2$ remains in diffusion equilibrium. The data used were those for which the corresponding value of $K_p'$ was in the range 3-4 and were selected without regard to hemisphere, season or any other consideration.

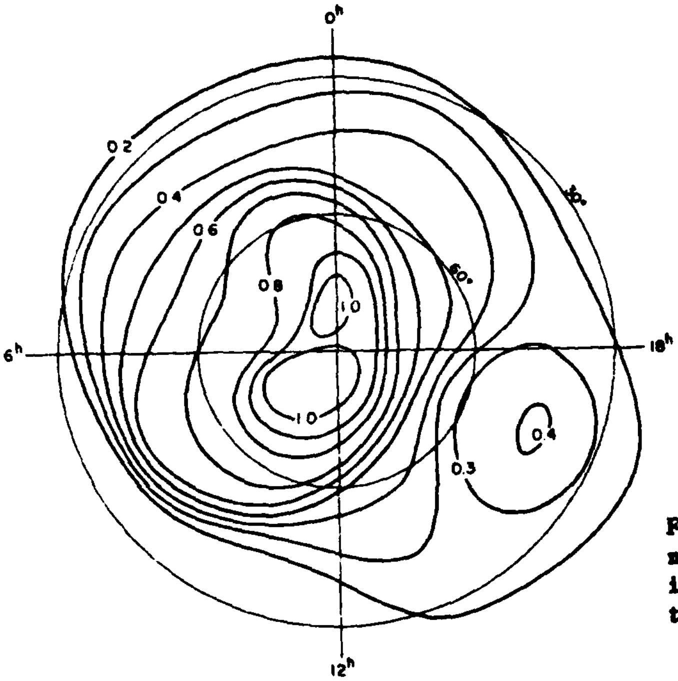


Figure 4. Isotherms of the normalized relative temperature increase derived from $N_2$ densities for $K_p$' in the range 3-4.

As can be seen from the figure, the response of the atmosphere to geomagnetic perturbation is generally much greater in the night and morning sectors than it is elsewhere. This confirms the trend found by Roemer (1971) from orbital-drag data as well as the findings of Taeusch (1977) and Prölss and von Zahn (1978) from gas analyzer data. The maximum in the morning sector is probably the same day-side heating zone previously detected in the ESRO 4 data by Fricke et al. (1974) and Raitt et al. (1975) and shown to move towards lower latitudes as the level of disturbance increases. It is probably associated, at least in part, with heating due to particle precipitation in the vicinity of the polar cusp. The enhancement in high latitudes in the night sector, on the other hand, is probably associated with joule dissipation in the westward electrojet system. The component of that electrojet that flows in the auroral oval in the evening sector is not so intense. The relatively steep temperature gradient there and, especially, at high latitudes in the afternoon sector may also be due in part to strong sunward winds in those regions. The mid-latitude enhancement throughout the night side has been shown by Raitt et al. (1975) to be closely correlated with zones of high-energy electron flux. Anti-sunward winds and waves generated in high latitudes may also be a factor here and in the morning sector as well, however. The secondary maximum in mid-latitudes in the afternoon sector, for which there yet seems to be no other explanation, may also be related to the wind system generated by the high latitude heat input.

Of course, the data of Figure 4 provide only a portion of the information needed to model the local time effects in detail. We must obtain similar information regarding the variations of the other constituents, not only at 80 km but at other heights as well. And, we must know how these distributions vary temporally and with the intensity of disturbance. It is also clear that the development of a model to fit these data will require a rather thorough understanding of the underlying physical processes.

## 5. REFERENCES


Champion, K. S. W., F. A. Marcos, and J. P. McIsaac, 1970. Atmospheric density measurements by research satellite OV1-15. Space Research V, North-Holland Publ. Co., Amsterdam, 450-458.

DeVries, L. L., 1972. Analysis and interpretation of density data from the low-g accelerometer calibration system (Logacs). Space Research XII, Akademie-Verlag, Berlin, 777-789.

Fricke, K. H., H. Trinks, and U. von Zahn, 1974. EOS Trans. AGU 55:370 (abstract).

Fuller-Rowell, T. J., and D. Rees, 1981. A three-dimensional, time-dependent simulation of the global dynamical response of the thermosphere to a geomagnetic substorm. J. Atmos. Ter. Phys. 43:701-721.

Hays, P. B., and R. G. Roble, 1976. Direct observations of thermospheric winds during geomagnetic storms. J. Geophys. Res. 76:5316-5321.

Hedin, A. E., H. G. Mayr, C. A. Reber, N. Spencer, and G. R. Carignan, 1974. Empirical model of global temperature and composition based on data from the OGO 6 quadrupole mass spectrometer. J. Geophys. Res. 79:215-225.

Hedin, A. E., J. E., Salah, J. V. Evans, C. A. Reber, G. P. Newton, N. W. Spencer, D. C. Kayser, D. Alcayd, P. Bauer, L. Cogger, and J. P. McClure, 1977a. A global thermospheric model based on mass spectrometer and incoherent scatter data; MSIS 1, $N_2$ density and temperature. J. Geophys. Res. 82:2139-2147.

Hedin, A. E., C. H. Reber, G. P. Newton, N. W. Spencer, H. C. Brinton, and H. G. Mayr, 1977b. A global thermospheric model based on mass spectrometer and incoherent scatter data; MSIS 2, Composition. J. Geophys. Res. 82:2148-2156.

Hedin, A. E., C. A. Reber, N. W. Spencer, H. C. Brinton, and D. C. Kayser, 1979. Global model of longitude/UT variations in thermospheric composition and temperature based on mass spectrometer data. J. Geophys. Res. 84:1-9.

Hedin, A. E., N. W. Spencer, H. G. Mayr, and H. S. Porter, 1981. Semiempirical modeling of thermospheric magnetic storms. J. Geophys. Res. 86:3515-3518.

Jacchia, L. G., 1959. Corpuscular radiation and the acceleration of artificial satellites. Nature 183:1662.

Jacchia, L. G., 1961. Satellite drag during the events of November 1960. Space Research II, North-Holland Publ. Co., Amsterdam, 747-750.

Jacchia, L. G., 1972. Atmospheric models in the region from 110 to 2000 km. CIRA 1972, Akademie-Verlag, Berlin, 341-396.

Jacchia, L. G., 1977. Thermospheric temperature, density, and composition: new models. Smithsonian Astrophys. Obs. Spec. Rep. No. 375, 106 pp.

Jacchia, L. G., and J. Slowey, 1963. An analysis of the atmospheric drag of the Explorer IX satellite from precisely reduced photographic observations. Space Research IV, North-Holland Publ. Co., Amsterdam, 257-270.

Jacchia, L. G., and J. Slowey, 1964a. Atmospheric heating in the auroral zones: a preliminary analysis of the atmospheric drag of the Injun 3 satellite. J. Geophys. Res. 69:905-910.

Jacchia, L. G., and J. Slowey, 1964b. Temperature variations in the upper atmosphere during geomagnetically quiet intervals. J. Geophys. Res. 69:4145-4148.

Jacchia, L. G., J. Slowey, and F. Verniani, 1967. Geomagnetic perturbations and upper atmospheric heating. J. Geophys. Res. 72:1423-1434.

Jacchia, L. G., J. W. Slowey, and U. von Zahn, 1976. Latitudinal changes in composition in the disturbed thermosphere from ESRO 4 measurements. J. Geophys. Res. 81:36-42.

Jacchia, L. G., J. W. Slowey, and U. von Zahn, 1977. Temperature, density, and composition in the disturbed thermosphere from ESRO 4 gas analyzer measurements: a global model. J. Geophys. Res. 82:684-688.

Jacchia, L. G. and J. Slowey, 1981. Analysis of data for the development of density and composition models of the upper atmosphere. AFGL-TR-81-0230, 20 pp.

Meng, C.-I., 1982. Latitudinal variation of the polar cusp during a magnetic storm. Geophys. Res. Lett. 9:60-63.

Newton, G. P., D. T. Pelz, and H. Volland, 1969. Direct in situ measurements of wave propagation in the neutral thermosphere. J. Geophys. Res. 74:183-196.

Porter, H. S., H. G. Mayr, and A. E. Hedin, 1981. An analytic formulation for heating source memory in the thermospheric composition. J. Geophys. Res. 86:3555-3560.

Prölss, G. W., 1980. Magnetic storm associated perturbations of the upper atmosphere: recent results obtained by satellite-borne gas analyzers. Rev. Geophys. Space Phys. 18:183-202.

Prölss, G. W., and K. H. Fricke, 1976. Neutral composition changes during a period of increasing magnetic activity. Planet. Space Sci. 24:61-67.

Prölss, G. W., and U. von Zahn, 1978. On the local time variation of atmospheric-ionospheric disturbances. Space Research XVIII 159-162, 1978.

Raitt, W. J., U. von Zahn, and P. Christopherson, 1975. A comparison of thermospheric neutral gas heating and related thermal and energetic plasma phenomena at high latitudes during geomagnetic disturbances. J. Geophys. Res. 80:2277-2288.

Roemer, M., 1971. Geomagnetic activity effect on atmospheric density in the 250 to 800 km altitude region. Space Research XI, Akademie-Verlag, Berlin, 965-974.

Roemer, M., 1972. Recent observational results on the thermosphere and exosphere. CIRA 1972, Akademie-Verlag, Berlin, 341-396.

Slowey, J. W., 1981. Models of the geomagnetic effect in the earth's thermosphere. Adv. Space Res. 1:213-219.

Smith, L. B., 1968. An observation of strong thermospheric winds during a geomagnetic storm. J. Geophys. Res. 73:4959-4963.

Taeusch, D. R., 1977. Structure of electrodynamic and particle heating in the disturbed polar thermosphere. J. Geophys. Res 82:455-460.

Taeusch, D. R., G. R. Carignan, and C. A. Reber, 1971. Neutral composition variation above 400 kilometers during a magnetic storm. J. Geophys. Res. 76:8313-8325.

von Zahn, U., W. Köhnlein, K. H. Fricke, U. Laux, H. Trinks, and H. Volland, 1977. ESRO 4 model of global thermospheric composition and temperatures during times of low solar activity. Geophys. Res. Lett. 4:33-36.